Journal of Thermal Analysis and Calorimetry, Vol. 83 (2006) 3, 617–623

EMANATION THERMAL ANALYSIS STUDY OF Na-MONTMORILLONITE AND MONTMORILLONITE SATURATED WITH VARIOUS CATIONS

V. Balek[1,2*], *M. Beneš*[2], *Z. Málek*[1], *G. Matuschek*[3], *A. Kettrup*[4] *and S. Yariv*[5]

[1]Nuclear Research Institute Řež, plc., 250 68 Řež, Czech Republic
[2]Research Center Řež, Ltd., 25068 Řež, Czech Republic
[3]GSF-Institute of Environmental Chemistry, Neuherberg, 8795 Oberschleissheim, Germany
[4]Department of Biosciences, Technical University Munich, 8795 Freising, Germany
[5]Department of Inorganic and Analytical Chemistry, The Hebrew University of Jerusalem, Jerusalem 91904, Israel

Emanation thermal analysis (ETA) and thermogravimetry measured in the range 20–1000°C was used to characterize the thermal behaviour of Na-montmorillonite (Upton Wyoming, USA) and homoionic montmorillonite samples prepared by saturation with cations Li^+, Mg^{2+}, Al^{3+}, respectively. It was confirmed that the presence of cations used for montmorillonite saturation (Li^+, Mg^{2+}, Al^{3+}) influenced the thermal behaviour of the samples. The results that indicated the decrease of radon release rate corresponding to a collapse of the interlayer space between the silicate sheets after water release and the crystallization of meta-montmorillonite in the respective temperature intervals were compared. From the ETA results it followed that the thermal stability of intermediate microstructure depends on the type of exchanged cation. A mathematical model was used to evaluate the ETA data.

Keywords: *emanation thermal analysis, meta-montmorillonite, microstructure, Na-montmorillonite, saturation with Li^+, Mg^{2+}, Al^{3+}, thermal behaviour, thermogravimetry*

Introduction

It is well known that the ion exchange of natural cations present in bentonite clays, like montmorillonite clay mineral (MMT), may influence their structure as well as their dehydration and dehydroxylation behaviour [1–3]. Differences in the dehydration are due to a more or less strong polarising power of the exchangeable cation. The hydration number of the exchangeable cations can be expressed by the basic spacing of the clay structure characterised by *c*-axis basal spacings d_{001} [3]. Changes of microstructure that accompany the dehydration and dehydroxylation of the MMT samples may be strongly affected by the ion exchange process [1, 2, 4, 5]. The decrease of *c*-axis basal spacing take place as the result of the dehydration (observed in the temperature range up to 200°C). Microstructure changes, that accompany the dehydroxylation process, have been described as the formation of amorphous meta-montmorillonite, rich in lattice vacancies.

In order to understand the environmental behaviour the natural and ion exchanged clay minerals a detailed study of microstructure changes that accompany the dehydration and dehydroxylation of the MMT, as affected by the saturation with various cations, has to be carried out. Moreover, it was of interest to investigate processes of the formation of amorphous meta-montmorillonite, as well as the healing of amorphous particles, that take place on further heating of the samples.

In this study the effect of Na-montmorillonite saturation with cations Li^+, Mg^{2+} and Al^{3+}, respectively on the formation of dehydrated products was characterized. TG/DTG measurements were used to characterize the dehydration and dehydroxylation processes.

By using X-ray diffraction *c*-axis basal spacing parameters of the montmorillonite samples were determined. Emanation thermal analysis (ETA) [6, 7], based on the measurement of radon release from the samples previously labelled, was used to monitor microstructure changes taking place during in situ heating of the samples saturated with the various cations.

ETA was already advantageously used in the characterization of various natural and synthetic minerals, e.g. natural vermiculite, synthetic hydrotalcite-like minerals, synthetic gibbsite, perovskite and others [8–12].

Experimental

Sample preparation

Na-montmorillonite (Upton, Wyoming, USA) was used as a starting material. Following experimental procedure was used for the preparation of the samples of homoionic montmorillonite saturated with Li^+, Mg^{2+} and Al^{3+} ions, respectively. For every ion exchange

* Author for correspondence: bal@ujv.cz

1388–6150/$20.00

Akadémiai Kiadó, Budapest, Hungary
Springer, Dordrecht, The Netherlands

sample the amount of 10 g of the Na-montmorillonite was mixed with 800 mL of water and stirred during two days. After decantation the amount of 200 mL of 0.2 M solution containing chlorides of respective cation was added. The suspension was stirred for two days, several times washed by distilled water until the negative reaction for chlorides (using Ag^+ ions). The products were air dried at the temperature of 40°C.

Methods

TG/DTG measurements were carried out using Netzsch STA 429 device on heating in nitrogen at the rate 5 K min^{-1}. ETA measurements were carried out using the upgraded Device for ETA-DTA by Netzsch Type 404. The samples were heated at the rate of 5 K min^{-1}, being overflowed by a constant flow of argon (50 mL min^{-1}) which carried the released radon atoms into the radioactivity detection chamber. In ETA [6, 7] the samples were labelled by impregnation with the acetone solution containing traces of nitrates of ^{228}Th and ^{228}Ra. The specific activity of the sample was 10^4 Bq g^{-1} atoms of radon ^{220}Rn were formed by the spontaneous α-decay of ^{228}Th and ^{224}Ra absorbed on the sample surface.The recoil depths of ^{224}Ra and ^{220}Rn ions implanted by the recoil (energy 85 keV/atom) into the subsurface of the samples were calculated by means of the TRIM code [13]. It was estimated that the radon atoms penetrated into the subsurface layers to a maximum depth of 80 nm. More details about ETA as a less common method are given elsewhere [6, 7]. XRD equipment (Philips PW 1050/25) using CuK_α Ni-filtered radiation was applied to obtain the XRD patterns and to determine the *c*-axis basal spacings (d_{001}).

Results and discussion

Thermogravimetry results of Na-MMT and homoionic MMT samples saturated with Li^+, Mg^{2+} and Al^{3+} ions, respectively are compared in Fig. 1. Table 1 presents an overview of the mass changes corresponding to samples dehydration and dehydroxylation. In the temperature range of about 20–200°C a water loss (mainly interlayer water situated between the silicate sheets)

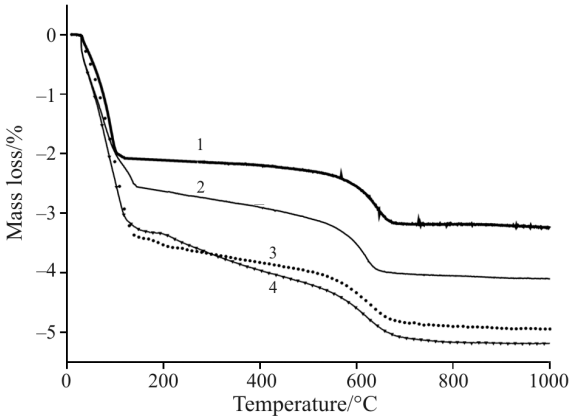

Fig. 1 Thermogravimetry results of montmorillonite samples measured during heating at the rate 5 K min^{-1}; 1 – Na-montmorillonite (Upton, Wyoming, USA), 2 – Li^+-exchanged montmorillonite, 3 – Mg^{2+}-exchanged montmorillonite, 4 – Al^{3+}-exchanged montmorillonite

took place. The mass loss observed at temperatures ranging between 200–700°C corresponds to the water release originating from OH groups structurally bound in the lattice. The temperature intervals of the water release corresponding to these processes as well as the amount of water released is dependent upon the nature of adsorbed cations and the hydration of surface. TG results presented in this study agree well with findings of other authors [14–18].

Mackenzie [14] suggested that the amount of interlayer water depends on hydration energy of the adsorbed cations and on hydration of the surface, and that TG curves can be interpreted to give relative values for these amounts of water. He stated that for most of divalent cations (e.g. Mg^{2+} and Ca^{2+}) the ion is more important that the interlayer surface, but for larger divalent cations as well as for monovalent cations the influence of the layered surface on the hydration is dominant. Glasser *et al*. [15] showed that the polyvalent ions tend to detach themselves from the silicate surface and incorporate in the water layers. They stated that the complete loss of the interlayer water is accompanied by a reduction in the *c*-axis dimensions (to 9.4–10 Å) with exact value depending on the size of interlamellar ions.

Table 1 Mass loss during dehydration and dehydroxylation of the montmorillonite samples saturated with various cations

Sample	Dehydration		Dehydroxylation	
	temperature range/°C	mass loss/%	temperature range/°C	mass loss/%
Na-MMT (initial sample)	20–100	7.23	450–680	4.14
Li-MMT	50–150	6.19	400–640	3.63
Mg-MMT	50–180	10.50	180–700	2.28
Al-MMT	50–120	6.37	120–650	5.22

Moreover, it is to mention that the TG results in this study agreed with the findings of Ferrandis *et al*. [16] who gave the following sequence for the rate of the hydroxyl loss for montmorillonites with exchanged cations: Li>K>Na>Mg>Ba>Ca>Sr. According to Bradley and Grim [17] the removal of hydroxyl water is correlating with increases of 0.1–0.3 Å in *c*-axis and involves the expulsion of about one sixth of the oxygen of the octahedrically co-ordinated positions of the structure resulting in the creation of lattice vacancies. Heller and Kalman [18] supposed that lithium and magnesium enter the vacant octahedral positions of dioctahedral forms during dehydroxylation.

The values of *c*-axis basal spacing (d_{001}) of montmorillonite samples that we have determined by XRD are [in Å] for Na-MMT: 12.399, for Li-MMT: 12.565, for Mg-MMT: 14.965, and for Al-MMT: 14.965. These data can be used for the characterisation of the hydration number and the binding of water in the respective samples. These values agree fairly well with the *c*-axis basal spacing values published by Rowland *et al*. [1]. They stated that the montmorillonite with sodium or potassium ions has a regular one water layer configuration as 12.4 Å. On the contrary the montmorillonite with calcium, magnesium, manganese, lithium and hydrogen cations have octahedral co-ordination of their exchange cations.

In Fig. 2 we present ETA results of Na-montmorillonite and homoionic montmorillonite samples prepared by saturation of Na-montmorillonite with Li^+, Mg^{2+} and Al^{3+} ions, respectively.

Microstructure changes characterized by ETA revealed differences in thermal behaviour of the samples (Fig. 2). The decrease of the radon release rate measured by ETA in the temperature range 120–200°C characterized changes of the interlayer space, filled initially by water molecules and the subsequent sticking of the interlayers. Figures 3a–d present a comparison of ETA and TG results of each of the montmorillonite samples investigated in this study. As it follows from the findings of other authors [16, 17] the release of interlayer water took place with all the ion-exchanged montmorillonite samples investigated in the temperature interval of 50–180°C. We assumed that the enhanced radon release rate observed was due to the surface exposure after the water release from the sample. The decrease of the radon release rate measured by ETA in the temperature interval 120–200°C characterized the decrease of the interlayer space, filled initially by water molecules and the subsequent sticking of the interlayers. The dehydroxylation of Na-montmorillonite and the ion-exchanged montmorillonite samples started at different temperatures, ranging from 180 to 450°C. The final temperatures of the mass decrease were ranging from 640 to 700°C (Table 1).

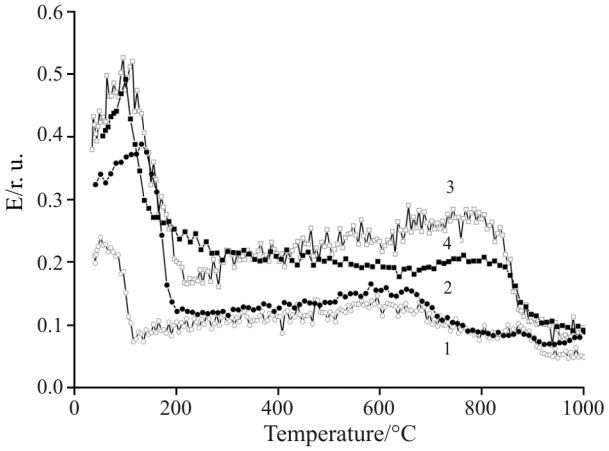

Fig. 2 ETA results of montmorillonite samples measured during heating at the rate 5 K min^{-1}; 1 – Na-montmorillonite (Upton, Wyoming, USA), 2 – Li^+-exchanged montmorillonite, 3 – Mg^{2+}-exchanged montmorillonite, 4 – Al^{3+}-exchanged montmorillonite

From ETA curves, it followed that the release of the structurally bound hydroxyl group was accompanied in some cases by an increase of radon release rate *E*, due to the formation of additional structure defects in the MMT samples, that served as radon diffusion channels. The increase of *E* is in agreement with the statement by Bradley *et al*. [17] that the removal of OH groups was connected with the creations of vacancies and an increase of *c*-axis structure parameter. It was supposed that after the dehydroxylation waste terminated (at temperatures 680–700°C for all MMT samples) a formation of meta-MMT structure took place.

A decrease of radon release rate *E* observed on further heating indicated the crystallisation of meta-MMT phases. According to the ETA results (Fig. 2) the crystallisation processes was different for the ion-exchanged montmorillonite samples investigated in this study. In order to evaluate the microstructure changes from ETA data mathematical model proposed by Beckman and Balek [18] was used. ETA experimental data are presented in Figs 3a–d as points, whereas model curves obtained by fitting the mathematical model [18] with the ETA experimental data are presented as full lines. A good agreement of the modelling results and experimental ETA data was achieved.

Modeling of ETA results

In modeling ETA data it was supposed that metastable structures may be formed on heating of the samples considerably varying in the number of diffusion paths available for the radon release from the sample. In order to evaluate ETA results obtained during heating of the samples different mechanisms for radon diffusion in solids were considered [18].

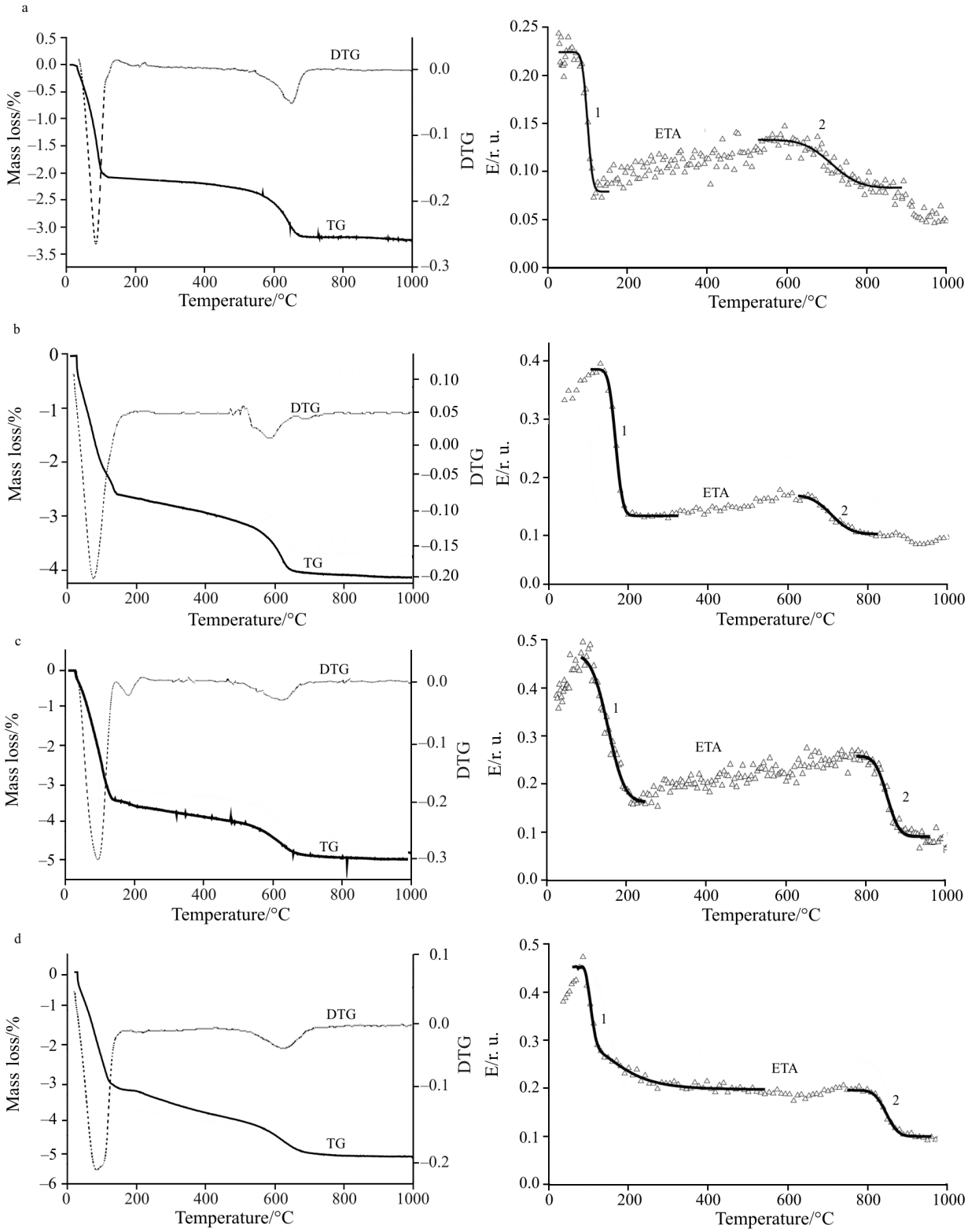

Fig. 3 Results of TG/DTG and ETA characterizing thermal behaviour of montmorillonite sample. Experimental data are presented by points Model curves obtained by fitting experimental ETA data with temperature dependences of $\Psi_i(T)$ are denoted as curves 1 and 2; a – Na-montmorillonite original sample (Upton, Wyoming, USA), b – Li^+-exchanged montmorillonite, c – Mg^{2+}-exchanged montmorillonite, d – Al^{3+}-exchanged montmorillonite

The release rate of radon from the sample, called also emanation rate, E, can expressed in a simplified way as follows [6, 7]:

$$E_{total}=E_R+E_D(T)\Psi(T) \quad (1)$$

where E_R is the emanation rate due to recoil, which depends on external surface area and radon recoil path in the respective solid, E_D is the emanation rate due to radon diffusion, which depends on the number of the diffusion paths serving for the radon release from the sample, $\Psi(T)$ is a function that describe the healing of the subsurface defects serving as paths for radon diffusion. The function $\Psi(T)$ can be used [18] for the description of the microstructure changes in the solid and the healing of structure defects that serve as channels for radon diffusion in the sample.

Equations (2)–(5) were used in the evaluation of the ETA experimental results. The temperature dependences of the function $\Psi(T)$ were used to describe the healing of structure defects that can serve as channels for radon diffusion in the sample [18]. Following expression was used for modelling the temperature dependence of E_D

$$E_D(T)=(3/y)\coth y-(1/y) \quad (2)$$

$$(1/y)=(S/M)\rho/(D/\lambda)^{1/2}$$

where (S/M) is the surface area of open pores, inter-granular space and of interfaces serving as radon diffusion paths, ρ is density of the sample, $(D/\lambda)^{1/2}=L_D$ is the average radon diffusion length. D is radon diffusion coefficient and λ is the radon decay constant ($\lambda=0.0127$ s^{-1}).

$D=D_0\exp(-Q/RT)$, where D_0 is the pre-exponential factor proportional to the number of structure defects serving as traps for radon atoms, Q is activation energy of radon migration involving both the activation energy of radon escape from the traps in the sample and that of the radon migration along diffusion path, R is molar gas constant ($R=8.31441$ J mol^{-1} K^{-1}), T is temperature in absolute Kelvin scale.

Following equations were used in the modeling of the temperature dependences of the radon release from the solid. Equation (3) was proposed for $\Psi(T)$ function to describe a decrease the subsurface defect as served as radon diffusion paths.

$$\Psi(T)=1-0.5\left[1+\mathrm{erf}\left(\frac{1-\frac{T_m}{T}}{\frac{\Delta T\sqrt{2}}{T}}\right)\right] \quad (3)$$

The increase of the radon release from the sample with temperature was described by Eq. (4)

$$E(T)=p3\,p1\exp\left(-\frac{p2}{T}\right)\cdot\left\{\coth\left[\frac{3}{p1\exp\left(-\frac{p2}{T}\right)}\right]-\frac{p1\exp\left(-\frac{p2}{T}\right)}{3}\right\} \quad (4)$$

The healing of structure defects that served as radon diffusion paths on sample heating was described by Eq. (5)

$$\Psi(T)=1-0.5\left[1+\mathrm{erf}\left(\frac{T-p4}{\sqrt{2}p5}\right)\right] \quad (5)$$

The value of diffusion coefficient that characterized the permeability of radon diffusion channels (transporting paths for the gas release) was determined by using Eq. (6)

$$D=p6\exp\left(-\frac{p7}{T}\right) \quad (6)$$

Parameters $p1\cdots p7$ were determined by fitting of the model curves with the experimental data of ETA.

Evaluation of the ETA results

As it follows from Figs 3a–d, the model curves used in this study fit well with the experimental data of ETA. The decrease of interlayer space that took place as the result of the dehydration as well as the crystallization of amorphous meta-MMT samples on heating up to 1000°C were characterized by ETA. The comparison of TG and ETA results, evaluated by the mathematical modelling brought about a more detailed information about processes that took place on heating of the ion-exchanged montmorillonite samples.

From values of the mass loss summarized in Table 1 it followed that the dehydroxylation of Na-montmorillonite and the ion-exchanged montmorillonite samples started at different temperatures, ranging from 180 to 450°C. The final temperatures of the mass decrease were ranging from 640 to 700°C.

From ETA curves it followed that the release of the structurally bound hydroxyl group was accompanied in some cases by an increase of radon release rate E, due to the formation of additional structure defects in the MMT samples, that served as radon diffusion channels. It has been supposed that after the dehydroxylation was terminated (at temperatures 680–700°C for all montmorillonite samples investigated in this study) the formation of meta-MMT structure took place.

On further heating, the crystallization of meta-MMT phases took place in slightly different temperature ranges. It was assumed that during the sample

heating a series of intermediate metastable structures was formed, considerably varying in the number of radon migration paths, in the permeability of radon diffusion paths as well as in the area of surface accessible for gas release. $\Psi(T)$ is a function that describe the temperature dependence of healing of the defects that served as channels for radon diffusion.

In Fig. 4 the temperature dependences of $\Psi(T)$ were used for the characterization of the collapse of the initial montmorillonite structure after dehydration as well as the nanostructure changes that accompanied the crystallization amorphous meta-MMT phases. The radon release measured served as nanostructure probe of the samples. We assumed that the decrease of radon mobility in the samples was due to the decrease of surface (porosity) and radon diffusion channels in the montmorillonite samples on their heating.

The respective temperature ranges of the collapse of the initial montmorillonite structure after dehydration and the crystallization of amorphous meta-MMT phases, that followed after dehydroxylation are summarised in Table 2. The onset temperatures of the annealing for ion-exchanged MMT samples were increasing in the following sequence:

Na-MMT<Li-MMT<Mg-MMT<Al-MMT

depicts temperature dependences of $\Psi(T)$ functions to be used for the characterization of (a) the collapse of the initial montmorillonite structure after dehydration and (b) the crystallization amorphous meta-MMT phases. Both processes were indicated by decrease of the radon release rate.

The most intense decrease of ΔE determined from the $\Psi(T)$ function corresponding to the collapse of the interlayer space was ascribed to the Mg-MMT sample. The *c*-axis basal spacing d_{001} determined for Mg-MMT sample in this study supported the results obtained by the evaluation of ETA results and presented in Table 2.

From Fig. 4a it followed that values of ΔE corresponding to the collapse of the interlayer space due to the dehydration of MMT samples increased in following sequence:

Na-MMT<Li-MMT≤Al-MMT<Mg-MMT

This is agreement with the values of *c*-axis basal spacing d_{001} mentioned this study for the respective samples.

Moreover, from Fig. 4b it followed that the values of ΔE corresponding to the crystallization of meta-MMT increased in the sequence:

Na-MMT<Li-MMT<Al-MMT<Mg-MMT

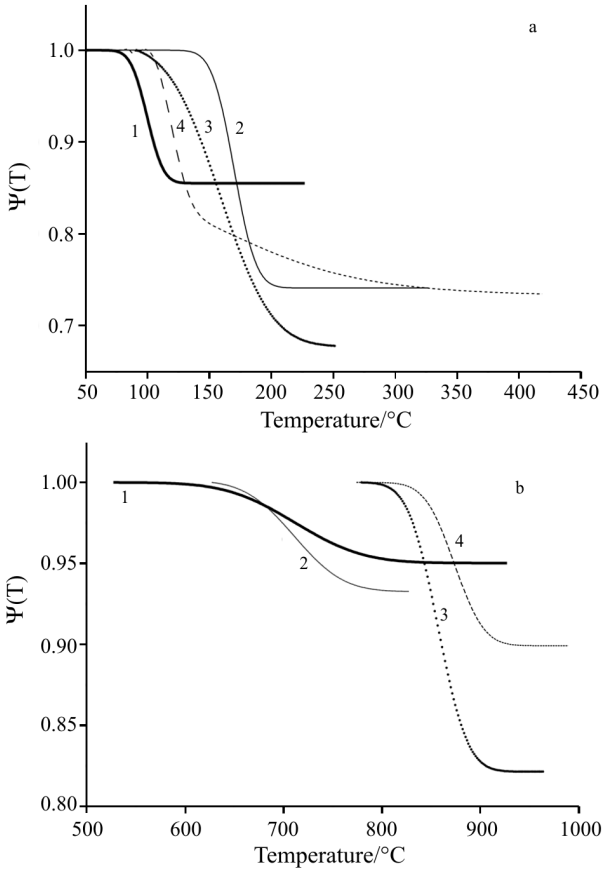

Fig. 4 Temperature dependences of $\Psi_i(T)$ functions characterizing; a – collapse of the interlayer space between the silicate sheets due to water release and b – the crystallization of meta-montmorillonite phases; 1 – Na-montmorillonite (Upton, Wyoming, USA), 2 – Li^+-exchanged montmorillonite, 3 – Mg^{2+}-exchanged montmorillonite, 4 – Al^{3+}-exchanged montmorillonite

Table 2 Microstructure changes that accompanied dehydration of montmorillonite and crystallization of meta-montmorillonite as determined from ETA results and $\Psi(T)$ functions

Sample	Dehydration			Crystallization of meta-montmorillonite		
	Temperature range/°C			Temperature range/°C		
	ETA model – curve 1			ETA model – curve 2		
	onset	final	ΔE	onset	final	ΔE
Na-MMT	60	140	0.15	620	810	0.05
Li-MMT	80	210	0.26	630	800	0.07
Mg-MMT	80	250	0.33	780	920	0.17
Al-MMT	88	350	0.26	790	960	0.10

Table 2 summarizes the ΔE values determined from $\Psi(T)$ functions in the respective temperature ranges (Figs 4a and b) where the collapse due to dehydration of the initial structure of montmorillonite samples and the crystallization of amorphous meta-MMT phases, respectively, took place.

Conclusions

ETA data evaluated by the mathematical modelling brought about a more detailed information to that obtained by TG and XRD about processes that took place on heating of Na-montmorillonite sample prepared by saturation with Li^+, Mg^{2+} and Al^{3+}-ions, respectively. A decrease of radon release rate corresponding to a collapse of the interlayer space between the silicate sheets after water release and the crystallization of meta-montmorillonite samples was characterized by ETA. From the ETA results it followed that the thermal stability of intermediate microstructure depends on the type of exchanged cation.

The results characterizing the environmental behaviour of the montmorillonite clay samples are of special importance when considering bentonitic clays as a backfill in the storage or disposal of hazardous waste.

Acknowledgements

Preparation and presentation of this work was supported by the Ministry of Education of Czech Republic (Project INGO and MSM 2672244501).

References

1 R. A. Rowland, E. J. Weiss and W. D. Bradley, Nat. Acad. Sci. Publ., 456 (1956) 85.
2 C. M. Warshaw, P. E. Rosenberg and R. Roy, Clay Minerals Bull., 4 (1960) 113.
3 Z. Málek, V. Balek, D. Garfinkel-Shweky and S. Yariv, J. Thermal Anal., 48 (1997) 83.
4 J. W. Earley, I. H. Milne and W. J. McVeagh, Am. Mineral., 38 (1953) 770.
5 C. M. Earnest, in: W. Smykatz-Kloss and Slade S. J. Warne (Eds), Thermal Analysis in Geosciences, Springer Verlag 1991, pp. 288–312.
6 V. Balek and J. Tölgyessy, Emanation thermal analysis and other radiometric emanation methods, in: Wilson and Wilson (Eds), Comprehensive Analytical Chemistry, Part XIIC, Elsevier, Amsterdam 1984, p. 304.
7 V. Balek, J. Šubrt, T. Mitsuhashi, I. N. Beckman and K. Györyová, J. Therm. Anal. Cal., 67 (2002) 15.
8 L. A. Pérez-Maqueda, V. Balek, J. Poyato, J. L. Pérez-Rodríquez, J. Šubrt, I. M. Bountseva, I. N. Beckman and Z. Málek, J. Therm. Anal. Cal., 71 (2003) 715.
9 F. Kovanda, V. Balek, V. Dorničák, P. Martinec, M. Mašláň, L. Bilková, D. Kolousek and I. M. Bountseva, J. Therm. Anal. Cal., 71 (2003) 727.
10 T. Stanimirova, T. Hibino and V. Balek, J. Therm. Anal. Cal., accepted.
11 V. Balek, Z. Málek, M. Beneš, H. Mitamura, T. Banba, I. N. Beckman, I. N. Bountseva, H. Haneda and T. Mitsuhashi, J. Therm. Anal. Cal., 80 (2005) 423.
12 V. Balek, J. Šubrt, J. Rouquerol, P. Llewellyn, V. Zelenák, I. M. Bountsewa, I. N. Beckman and K. Györyová, J. Therm. Anal. Cal., 71 (2003) 773.
13 J. F. Ziegler and J. P. Biersack, The stopping and range of ions in solids, Pergamon Press, New York 1985.
14 R.C. Mackenzie, Ber. Deut. Keram. Ges., 41 (1964) 696.
15 R. I. Glasser, I. Mantin and J. Mering, Intern. Geol. Congr. 21st Session, Norden, France 1960, pp. 28–34.
16 V. A. Ferrandis and M. C. Rodríguez-Pascual, Anales Edafol. Fysiol. Vegetal (Madrid), 17 (1958) 257.
17 W. F. Bradley and R. E. Grim, Am. Mineral., 36 (1951) 182.
18 I. N. Beckman and V. Balek, J. Therm. Anal. Cal., 67 (2002) 49.
19 L. Heller and Z. H. Kalman, Clay Minerals Bull., 4 (1961) 213.

DOI: 10.1007/s10973-005-7424-y